14TH CANADIAN MASONRY SYMPOSIUM
MONTREAL, CANADA
MAY 16TH – MAY 20TH, 2021

PRE-TEST ANALYSIS OF THE EFFECT OF ROTATIONAL BASE STIFFNESS ON LOADBEARING SLENDER MASONRY WALLS

Alonso, Alan[1]; Gonzalez, Rafael[2]; Cruz, Carlos[3] and Tomlinson, Douglas[4]

ABSTRACT

Slender Masonry Walls (SMWs) with slenderness ratio over 30 are widely used in Canada in single-storey buildings. However, the design of these walls tends to have stringent limits and requirements by the Canadian masonry standard (CSA S304-14). One of those requirements is neglecting the base stiffness provided by the foundation despite the inherent rotational base stiffness at the wall base. This concern is based on the potential Plastic Hinge (PH) formation near to the base due to the concentrated rotational demand. Due to the limited information on this topic, there is a need to investigate the structural performance of SMWs by implementing the rotational base stiffness. Analytical simulation is used to obtain expected Out-Of-Plane (OOP) performance of SMWs with pinned base and different rotational base stiffness conditions, using a Finite Element (FE) model. To compare the SMWs performances, the same slenderness ratio, loads, and reinforcement ratio are used. This pre-test analysis was used to design the experimental setup and obtain the adequate loads for the specimens to be tested in the experimental stage. Moreover, the experimental results from the next stage together with the parametric analyses will generate design recommendations regarding permissible slenderness ratios, axial load levels and ductility requirements.

KEYWORDS: *analytical simulation, finite element, masonry walls, out of plane, slender walls*

[1] PhD Student, University of Alberta, 9211-116th St., Edmonton, AB, Canada, alonsori@ualberta.ca
[2] MSc Student, University of Alberta, 9211-116th St., Edmonton, AB, Canada, rafaelde@ualberta.ca
[3] Associate Professor, University of Alberta, 9211-116th St., Edmonton, AB, Canada, cruznogu@ualberta.ca
[4] Assistant Professor, University of Alberta, 9211-116th St., Edmonton, AB, Canada, dtomlins@ualberta.ca

INTRODUCTION

The design of masonry walls with slenderness ratio over 30 tends to have stringent limits by the Canadian masonry standard (CSA S304-14) [1]. Design provisions require a ductile behaviour with significant deformation before the crushing of the masonry and not a stability failure. To meet this performance, SMWs often require thicker blocks and more steel details that make them economically impractical. Moreover, the wall must be designed assuming a pinned condition at the base neglecting the rotational base stiffness provided by the foundation. This assumption is based on the expected degradation of the masonry near to the wall-base due to the concentrated rotational demand under cyclic loads. This simplification could lead to underestimate the real capacity of SMWs.

Since 1980, there has been no innovation in SMWs when the American Concrete Institute (ACI) and the Structural Engineers Association of Southern Californica (SEASC) created a Test Report on Slender Walls [2]. Thirty full-scale, reinforced concrete and masonry pinned-pinned walls were tested under combined axial and lateral load. Nine of the 30 panels were built using Concrete Masonry Units (CMU) with slenderness ratios of 29, 36, and 48. This report was used as a reference to develop the following Canadian masonry design standard (CSA S304.1 1-M94) until the current one (CSA S304-14) [1]. Therefore, it seems that the stringent limits placed on SMWs design codes comes from the ACI-SEASC report.

To achieve a superior structural performance on SMWs under OPP and gravity loads, Amrhein [3] proposed altering any of the following factors. Using higher-strength units, placing the rebar closer to the face-shell, and implementing the inherent rotational base stiffness from the proper connection between the wall and foundation. The implementation of rotational base stiffness when designing SMWs would increase the OOP stiffness, decreasing the lateral deflection and consequently reducing the second-order effects. This could lead to reductions in steel reinforcement or a reduction in the wall thickness. In many cases, SMWs with a slenderness ratio over 30 require a wall thickness up to 300 mm to comply with code requirements. Reducing the wall thickness to 200 mm or even 250 mm will lead to more economic wall designs while maintaining satisfactory strength and reliable structural performance.

Mohsin [4] was a pioneer in testing loadbearing tall walls simulating the rotational base stiffness provided by the foundations, since most of the studies were tested using a pin condition at the base. 8 full-scale SMWs were tested under an eccentric axial load, finding a significant reduction on the second-order effects and increment in the loadbearing wall capacity. Also, the effective flexural rigidity was obtained and compared with that calculated using the CSA S304.1, showing that conservative values are calculated by the Canadian standard. However, Mohsin's [4] study was limited to eccentric axial loads neglecting OOP loads. Therefore, Pettit [5] investigated the effect of the rotational base stiffness on masonry walls combining gravity and OOP loads. Four moderately slender masonry walls were tested, and it was concluded that the effect of the rotational base stiffness on loadbearing masonry walls increase the wall capacity. Nevertheless, these walls were not susceptible to second-order effects, the presence of which will decrease the wall capacity.

As a result of these previous studies, there is a need to compile, review, and process the data for SMWs generated in the last 40 years to take advantage of modern construction practices and obtain a better understanding of SMWs structural performance using a real rotational base stiffness. The first stage is this analytical study, obtaining the control specimen and the loads that will be used in the experimental stage. Moreover, the parametric analysis was conducted to compare the SMWs performance between the pinned base condition and the non-zero rotational base stiffness, using the same slenderness ratio, loads, and reinforcement ratio.

NUMERICAL MODEL

The numerical model was developed using the Open System for Earthquake Engineering Simulation (OpenSEES) open-source software [6]. A nonlinear Finite Element (FE) 2D model was created using a macro-modeling approach (Figure 1). This model consists of a tall wall subdivided into 30 nonlinear beam-column type elements using a fiber-section to apply distributed plasticity. The top of the wall is free in the Y direction and rotation while along the X direction is restrained (roller). However, the base of the wall is restrained in the X and Y while the rotation can be free or none-zero rotational stiffness (pinned).

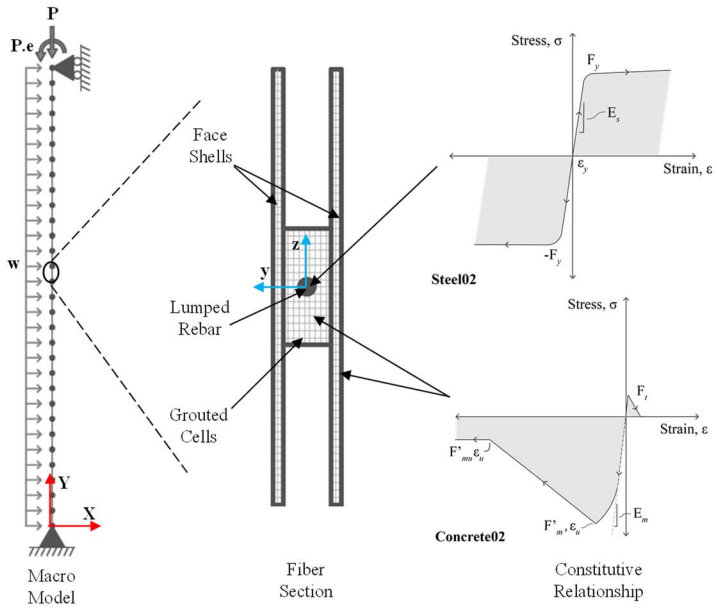

Figure 1: SMWs macro-model and fiber section with their respective constitutive relationship implemented (global axis: red; local axis: blue)

The material nonlinearity was reproduced using the uniaxial stress-strain models from the OpenSEES library. The longitudinal reinforcement was simulated using the material model *Steel02* with isotropic strain hardening based on the Guiffre-Menegotto-Pinto [7] model. The homogenous behavior of the masonry was simulated using the material model *Concrete02* based on the Kent-Scott-Park [8] model. The proposed model by Priestley and Elder [9] was adopted in this study to calculate the ultimate and crushing stress of the masonry fibres; the maximum compressive strength is assumed to happen at a strain of 0.002. Moreover, the maximum tensile

strength of the masonry was assumed to be 0.65 MPa, linear elastic until cracking and a linear tension softening.

The SMW macro-model is analyzed using a push-over analysis where an eccentric load is applied at the top of the wall, after the load is fully applied and sustained, the lateral load is applied along the height of the wall until the ultimate target displacement is achieved at midspan. The second-order effects are considered using the geometric transformation law available in the OpenSEES library (*Corotational transformation*). A zero-length element is used to recreate the rotational base stiffness when a non-zero base-stiffness is required.

Model Validation

Two experimental studies with different loading protocols were used to validate the model predictions. The first study used was the Test Report on Slender Walls [2] by the ACI-SEASC. Although this report was more than 40 years ago still being one of the most used as a reference on tall wall studies. Nine tall Fully Grouted (FG) reinforced-masonry walls were tested under an eccentric axial load on the top of the specimens and a uniform lateral pressure applied on one side of the wall using an airbag.

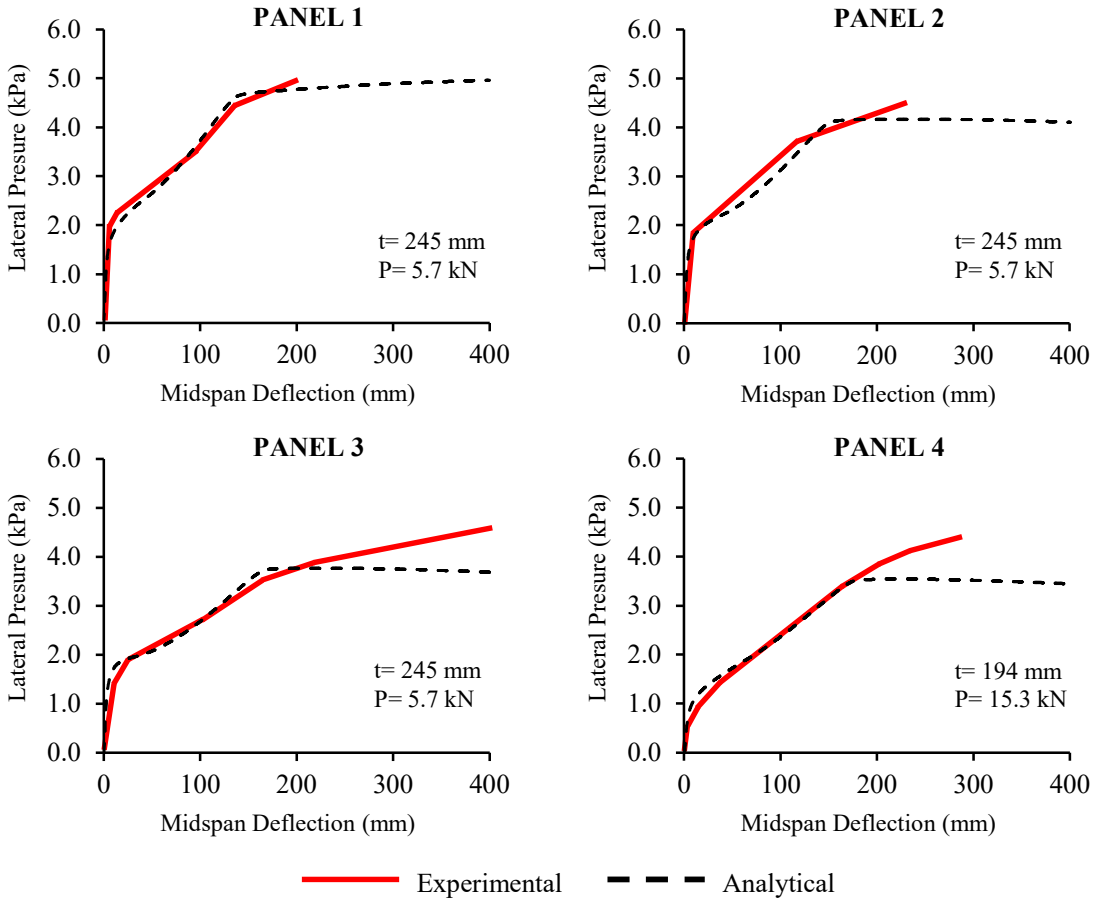

Figure 2: Model validation using the ACI-SEASC [2] experimental results

The second study used to validate the model was conducted by Mohsin [4] at the University of Alberta. Two groups of four Partially Grouted (PG) reinforced-masonry walls with different slenderness ratios (28.6 and 33.9) were tested under eccentric axial load on the top of the specimen.

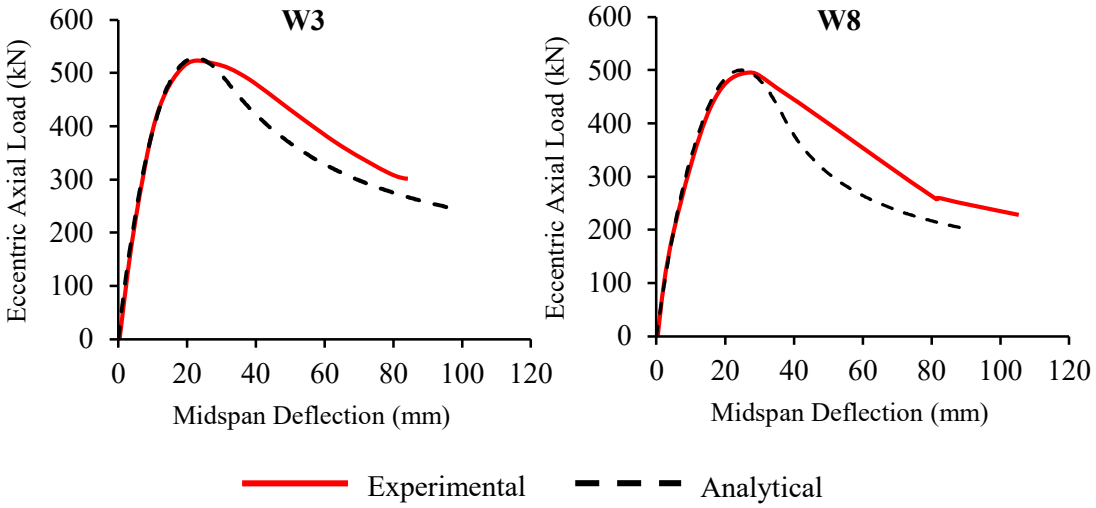

Figure 3: Model validation using Mohsin's [4] experimental results

In both cases, good correlation when comparing the experimental results against the model prediction is observed (Figure 2 and Figure 3).

CONTROL SPECIMEN ANALYSIS

A parametric analysis on the control specimen proposed for the experimental stage was conducted in this study. The objective of this was to obtain the optimal eccentric axial load to be applied because SMWs are susceptible to the second-order effects and can fail due to instability. Also, it is of great importance to establish a limit to stop the test because it could be dangerous if the SMW is tested until material failure.

The control specimen proposed was based on the specimens used by Pettit [5], using the same vertical and horizontal reinforcement, width, thickness, but different height (Figure 4). This geometry results in a slenderness ratio of 46, resulting in a larger value than the limit of 30 established by the CSA S304-14. Moreover, material properties were based on the same study [5]. The test was done in the Morrison Structural Laboratory at the University of Alberta and conducted in accordance with the Canadian standard. The masonry construction materials used are representative those in Alberta. For the masonry, the compressive strength obtained was f'_m= 16.8 MPa, the tensile strength was f_r = 0.65 MPa, and the maximum compressive strain of 0.002. For the steel reinforcement, the yield stress obtained was f_y = 533 MPa and Young's Modulus of E_s= 199 GPa. A value of *23.6* kN/m^3 as volumetric weight was used for the wall self-weight calculation, according to the information provided by Drysdale [10] in Appendix B.

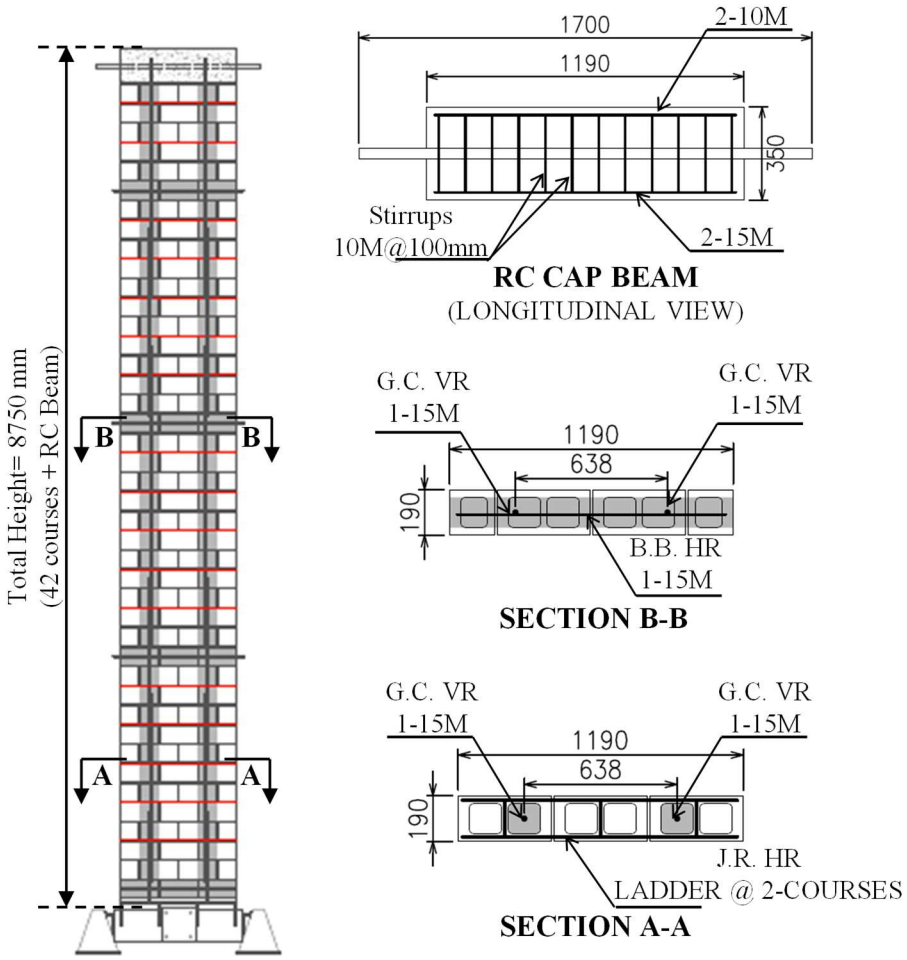

Figure 4: Control Specimen geometry and reinforcement (Units mm)

Eccentric axial load

A push-over analysis was applied to this SMW with a different eccentric axial load. A value of 170 mm as eccentricity was used, 20 mm of out-of-straightness at the middle of the wall was assumed due to possible imperfection during the construction of this tall wall. Pinned base condition was used to analyze the control wall.

Figure 5 shows the overall OOP capacity of the wall under different eccentric axial loads. It is evident that while the eccentric axial load increases, the maximum lateral pressure in the wall decreases. When the eccentric axial load increases from 5 kN to 15 kN, the maximum lateral pressure decreases by 25%. Meanwhile, with the increment of the eccentric axial load from 15 kN to 25 kN, the lateral pressure decreases 33%. Although the increment of the eccentric axial load of 10 kN was the same for the first and second scenarios, the percentage of decrease was different between them. Finally, when the eccentric axial load applied is 50 kN, the wall reached 0.22 kPa of maximum lateral pressure before failing due to instability. This is because SMWs are susceptible to the second-order effects and buckle before material failure.

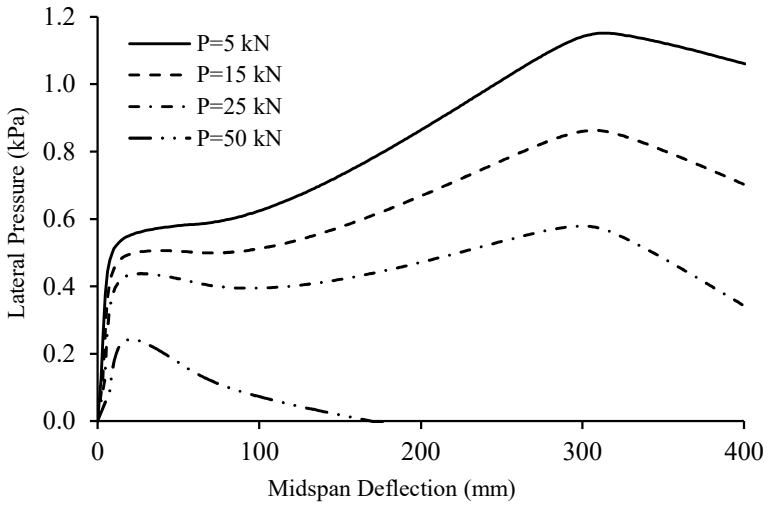

Figure 5: Capacity curve under different eccentric axial loads

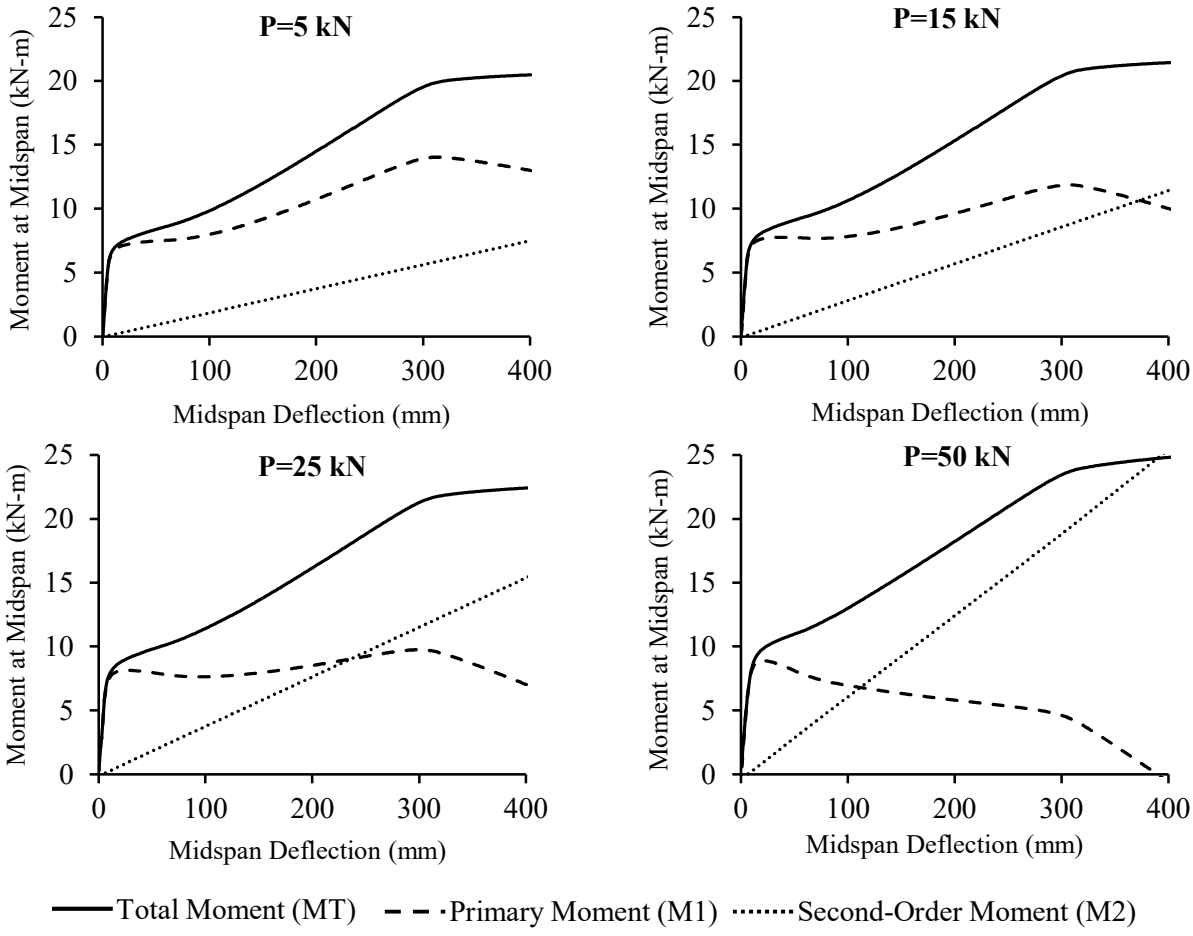

Figure 6: Moment interaction under different eccentric axial loads at midspan

Primary and Second-Order Moment interaction

To get a better understanding of second-order effects in the control specimen, Figure 6 shows the interaction between the Primary Moment (M1) and the Second-Order Moment (M2) to form the Total Moment (MT) versus the deflection at midspan. The first characteristic that can be noticed is when the eccentric axial load increases the slope of M2 also increases while M1 tends to decrease. In the first scenario when P= 5 kN, MT is composed mostly by M1 while M2 contributes with a lower percentage, but M2 constantly increases as the wall as well deforms without exceeding M1. The second scenario when P=15 kN, MT is still mainly composed by M1. However, after M1 reaches the maximum peak at 311 mm of midspan deflection as well as M2 still increasing up to 378 mm of deflection where M2 becomes greater than M1. The third scenario when P=25 kN, shows a similar behavior as the second scenario but in this case M2 becomes greater than M1 at 239 mm of midspan deflection before M1 reaches its maximum peak. Finally, the fourth scenario when P= 50kN, it is evident how the wall fails due to instability early when M1 reaches its maximum peak at 30 mm of midspan deflection. Therefore, first scenario the second-order effects are not significant, the second scenario presents second-order effects, and the wall is stable before the wall reaches its maximum lateral pressure. The third scenario also presents second-order effects but in this case are significant rather than in the second scenario, reaching values of M2 greater than M1 making the wall unstable before the wall reaches its maximum lateral pressure. The last scenario shows a typical instability failure, when M1 reaches its maximum peak early in the graph.

Results

As a result of this analysis, the value of 15 kN as the eccentric axial load was selected for the experimental stage. Moreover, it is recommended to stop the test at 311 mm of midspan deflection to avoid a sudden failure.

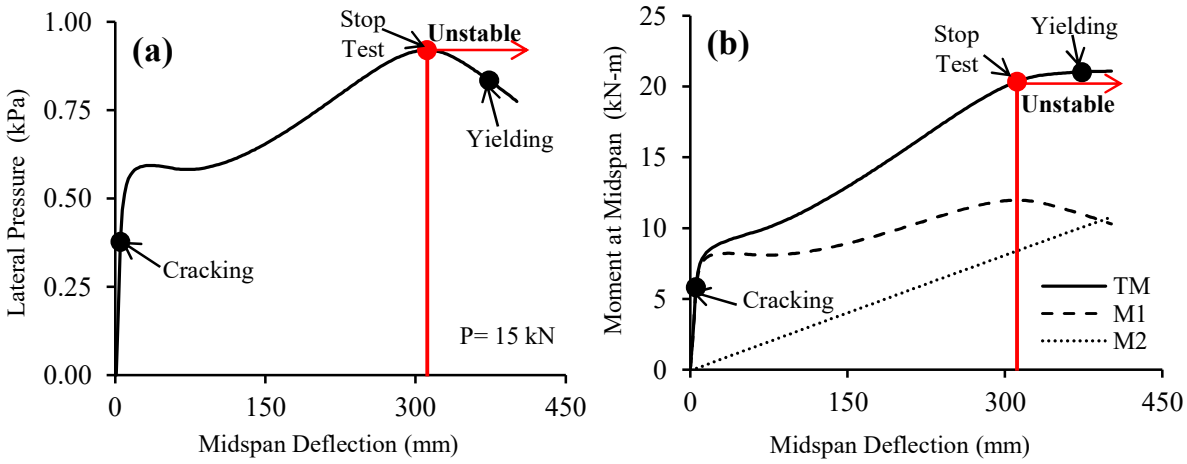

Figure 7: Midspan deflection at instability. (a) Capacity curve (b) M1 and M2 interaction

Figure 8 shows the deflected shape profile predicted at cracking, yielding, and at the proposed limit deflection before instability failure. Also, it is important to mention that crushing at masonry is not achieved under these boundary conditions and applied loading.

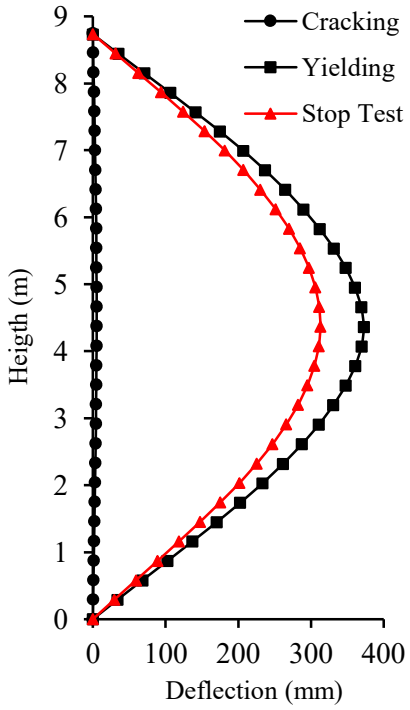

Figure 8: Deflection profile expected

ROTATIONAL BASE STIFFNESS EFFECT

To investigate the effect of the Rotational Base Stiffness (RBS) in the control specimen, three different RBS of 250, 500, and 1,000 kN-m/rad were used to compare the pinned-pinned and fixed-pinned conditions (RBS= 0 kN-m/rad and Infinite, respectively).

Figure 9 (a) shows the increment of the wall capacity while the RBS increases. When RBS = 250, 500, and 1,000 are applied, increments of 88, 120, and 131% can be observed in the maximum peak of lateral pressure. Moreover, it can be seen the yield displacement shifts among the five curves. That means that yield displacement decreases while RBS increases. After achieving the yield displacement, the capacity curves show a decrement, meaning in a drop of the OOP stiffness.

The deflected profiles with different RBS showed in Figure 9 (b) were plotted at the maximum peak of lateral pressure according to Figure 9 (a). When values of RBS = 250, 500, and 1,000 kN-m/rad are applied, decreases of 8, 9, and 18% of the maximum displacement can be observed, respectively. Although the differences in the maximum deflection were not significant with values of RBS = 250 and 500 kN-m/rad, a higher lateral pressure was required to achieve this maximum displacement in comparison to the pinned base condition. Moreover, the position of the maximum displacement is no longer the midspan when the RBS is present.

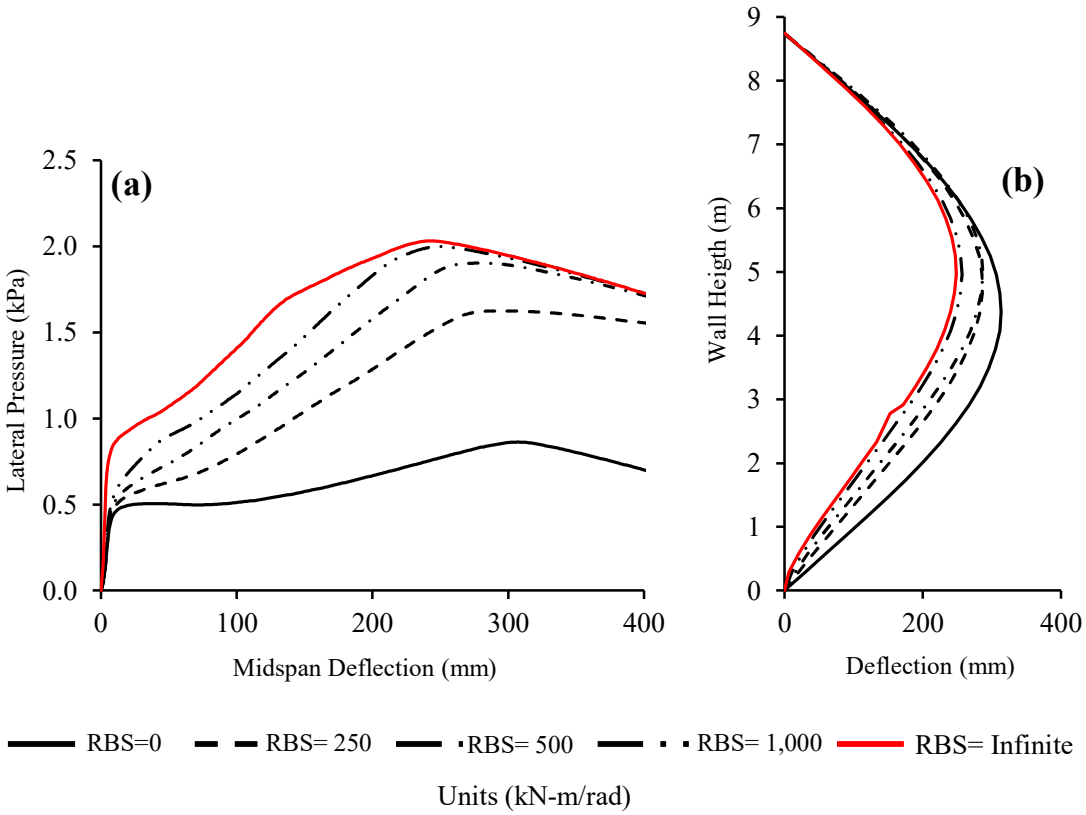

Figure 9: RBS comparison (a) Capacity Curve (b) Deflection profile

CONCLUSIONS AND FUTURE STUDIES

The macro model developed was able to predict the OOP performance of SMWs subjected to lateral and eccentric axial loads according to the experimental results used in the validation phase. A value of 15 kN as eccentric axial load was determined to be applied to the specimens during the experimental stage. Moreover, 311 mm was set as the maximum displacement to be achieved during the control specimen test to maintain the safety of the test. A similar analysis should be done for the specimens with RBS to set similar limits.

The OOP performance of SMWs under eccentric axial load and uniform lateral pressure appears to be significantly influenced by the RBS. Even with the smallest RBS value applied, the capacity increased 88% and the deflection decreased to 8%. However, the material degradation near to the base should be investigated to avoid sudden failures due to masonry crushing. A model with cyclic loading can be implemented to investigate this phenomenon.

The results from this analysis were used to design the control specimen and obtain the predicted behavior during the experimental stage. Also, the range of the RBS were determined for the other specimens. Moreover, the experimental results from the next stage together with the parametric analyses will generate design recommendations regarding permissible slenderness ratios, axial load levels and ductility requirements.

ACKNOWLEDGEMENTS

The authors wish to graciously acknowledge the generous contributions and donations from CONACYT, the Masonry Contractors Association of Alberta (MCAA), EXPOCRETE, the Canadian Masonry Design Centre (CMDC), and the Alberta Masonry Council (AMC).

REFERENCES

[1] Canadian Standards Association. *S304-14 Design of Masonry Structures*. Mississauga, ON, Canada.

[2] American Concrete Institute, and Structural Engineers Association of South California (1980). "Test Report on Slender Walls", Los Angeles, CA, United States.

[3] Amrheim, J. E. (1981) "Slender wall research by California Structural Engineers." *The Masonry Society Journal*., 1(2), 9-16.

[4] Mohsing, E. (2005). "Support Stiffness Effect on Tall Load Bearing Masonry Walls", PhD dissertation, University of Alberta. Edmonton, AB, Canada.

[5] Pettit, C.E.J. (2020). "Effect of Rotational Base Stiffness on the Behaviour of Loadbearing Masonry Walls", Master's thesis, University of Alberta. Edmonton, AB, Canada.

[6] McKenna, F., Scott, M. H., and Jeremic, B. (2000) "Open System for Earthquake Engineering Simulation (OpenSEES) [Computer Software]" *Pacific Earthquake Engineering Research Centre,* University of California. Berkeley, California, USA.

[7] Menegotto, M., and Pinto, P. E. (1973). "Method of analysis for cyclically loaded reinforced concrete plane force and bending." *Symposium on Resistance and Ultimate Deformability of Structures Acted on by Well Defined Repeated Loads,* IABSE, Lisbon, Portugal, 15-22.

[8] Kent, D. C., and Park, R. (1971). "Flexural members with confined concrete." *J. Struct. Div., ASCE*., 97: 1969-1990.

[9] Priestley, M. J. N., and Elder, D. M. (1983). "Stress-strain curves for unconfined and confined concrete masonry." *J. Proc.*, 80, 192-201.

[10] Drysdale, R. G. and Hamid, A. A. (2005). *Masonry Structures Behaviour and Design*, Canada Masonry Design Centre, Mississauga, ON, Canada.